S100A16 stabilizes the ITGA3-mediated ECM-receptor interaction pathway to drive the malignant properties of lung adenocarcinoma cells via binding MOV10

LIANREN YANG, AJUAN SHEN, RUJUN WANG and ZHIHUI ZHENG

Department of Medical Oncology, Taihe County People's Hospital, Fuyang, Anhui 236600, P.R. China

Received May 11, 2024; Accepted August 30, 2024

DOI: 10.3892/mmr.2024.13376

Abstract. Lung adenocarcinoma (LUAD) is highly associated with lung cancer-associated mortality. Notably, S100 calcium-binding protein A16 (S100A16) has been increasingly considered to have prognostic value in LUAD; however, the underlying mechanism remains unknown. In the present study, S100A16 expression levels in LUAD tissues and cells were respectively analyzed by the UALCAN database and western blotting. Cell Counting Kit-8 and 5-ethynyl-2'-deoxyuridine assays were used to examine cell proliferation, whereas wound healing, Transwell and tube formation assays were used to assess cell migration, invasion and angiogenesis, respectively. Western blotting was also used to examine the expression levels of proteins associated with metastasis, angiogenesis, focal adhesion and the extracellular matrix (ECM)-receptor interaction pathways. The relationship between S100A16 and Mov10 RNA helicase (MOV10) was predicted by bioinformatics tools, and was verified using a co-immunoprecipitation assay. Furthermore, the interaction between MOV10 and integrin α3 (ITGA3) was verified by RNA immunoprecipitation assay, and the actinomycin D assay was used to detect ITGA3 mRNA stability. The results demonstrated that S100A16 expression was increased in LUAD tissues and cell lines, and was associated with unfavorable outcomes. Knocking down S100A16 expression hindered the proliferation, migration, invasion and angiogenesis of LUAD cells. Furthermore, S100A16 was shown to bind to MOV10 and positively modulate MOV10 expression in LUAD cells, while MOV10 overexpression partially reversed the suppressive role of S100A16 knockdown on the aggressive phenotypes of LUAD cells. Furthermore, it was demonstrated that S100A16 regulated the stability of ITGA3 mRNA via MOV10 to mediate ECM-receptor interactions. In conclusion, S100A16 may bind to MOV10 to stabilize ITGA3 mRNA and regulate ECM-receptor interactions, hence contributing to the malignant progression of LUAD.

Correspondence to: Dr Zhihui Zheng, Department of Medical Oncology, Taihe County People's Hospital, 21 Jiankang Road, Taihe, Fuyang, Anhui 236600, P.R. China
E-mail: zhengzhihui_zh@163.com

Key words: angiogenesis, integrin α3, Mov10 RNA helicase, lung adenocarcinoma, S100 calcium-binding protein A16

Introduction

Lung cancer is one of the most common causes of cancer-related mortality both in China and globally; according to statistics, lung cancer accounts for 18.4% of tumor-associated deaths worldwide (1,2). Non-small cell lung cancer (NSCLC) is the predominant histopathological subtype of lung cancer, which is responsible for 80-85% of lung cancer cases (3). Lung adenocarcinoma (LUAD) represents the most prevalent and the most studied pathological type of NSCLC, and it accounts for approximately two-fifths of all lung cancer cases (4). Despite notable efforts to improve early detection and to develop new treatment methods, the prognosis of LUAD remains poor, mainly due to late diagnosis, metastasis and high postoperative recurrence rates (5-7). Therefore, improving understanding of the potential molecular mechanisms and the identification of novel candidate biomarkers of LUAD are critical to the development of novel diagnostic strategies and targeted therapies.

The S100 protein family, composed of small acidic proteins with an EF-hand Ca^{2+} binding motif, has been reported to perform functions in diverse tumor behaviors, such as cell proliferation, metastasis, angiogenesis and immune evasion (8). In particular, S100 calcium-binding protein A16 (S100A16), which is ubiquitously expressed in human tissues, has been well documented to be differentially expressed in the majority of human cancer types, where it functions in tumorigenic processes (9,10). Notably, S100A16 expression has been reported to be significantly upregulated in LUAD, and may be associated with poor overall survival and the efficacy of platinum-based adjuvant chemotherapy in LUAD (11,12). Moreover, a recent study suggested that S100A16, targeted by microRNA-508-5p, may participate in the proliferation and metastasis of LUAD cells (13). However, the mechanism of action of S100A16 in LUAD has not yet been determined and requires further evaluation.

Mov10 RNA helicase (MOV10) is a newly discovered RNA-binding protein (RBP) that belongs to the RNA helicase superfamily. It has previously been reported that MOV10 expression is 2-3 times higher in human Burkitt's lymphoma cells and cervical cancer cells than that in normal cells (14).

Furthermore, high MOV10 expression has been predicted to be related to poor prognosis in LUAD, according to the Kaplan-Meier plotter database (15). Notably, the ENCORI database (https://rnasysu.com/encori/) has predicted that the RBP, MOV10, may target the extracellular matrix (ECM)-related integrin α3 (ITGA3) mRNA, and ITGA3 may could be considered an independent prognostic marker of NSCLC (16).

The present study aimed to determine the role of S100A16 in LUAD, and to identify the S100A16-mediated mechanism in LUAD. The findings may provide a novel molecular mechanism involved in LUAD and thus improve understanding of the progression of LUAD.

Materials and methods

Bioinformatics tools. The Cancer Genome Atlas data in the UALCAN database (http://ualcan.path.uab.edu/index.html) were used to analyze S100A16 expression in LUAD tissues and performed survival analysis using log-rank test (17). BioGRID (https://thebiogrid.org/) and Pathway Commons databases (http://www.pathwaycommons.org/) were used to predict the downstream interacting proteins of S100A16. LinkedOmics database (https://www.linkedomics.org/login.php) was utilized to study the enrichment of S100A16 in the ECM-receptor interaction pathway. The ENCORI database (https://rnasysu.com/encori/) was used to predict the RNA-binding protein that could target MOV10.

Cell culture and treatment. The human bronchial epithelial cell line BEAS2B, the LUAD cell lines H1975, PC-9, A549 and HCC827, and human umbilical vein endothelial cells (HUVECs; fourth passage; cat. no. iCell-h110) were procured from Cellverse Bioscience Technology Co., Ltd. The cells were cultured in Dulbecco's Modified Eagle Medium (DMEM; Gibco; Thermo Fisher Scientific, Inc.), with the exception of HCC827 cells, which were cultured in Roswell Park Memorial Institute-1640 medium (Gibco; Thermo Fisher Scientific, Inc.). All cells were maintained in medium containing 10% fetal bovine serum (FBS; Gemini Bio Products), 100 U/ml penicillin and 100 μg/ml streptomycin in a 5% CO_2 humidified environment at 37˚C.

Plasmid transfection. S100A16 or MOV10 small interfering (si)RNAs [siRNA-S100A16 (5'-GCCAAATTCCTGCCTGATTCTGG-3') or siRNA-MOV10 (5'-ATGCTTCTTCAGGGAACAAGTAT-3')] and the scrambled siRNA [siRNA-negative control (NC): 5'-GCAACAAGATGAAGAGCACCAA-3'] were designed and produced by Shanghai Quanyang Biotechnology Co., Ltd. The MOV10 overexpression vector (Ov-MOV10) and the empty NC vector (Ov-NC) were synthesized by General Biosystems (Anhui) Corporation Ltd. The siRNAs or vectors (20 μM) were transfected into H1975 cells ($1x10^5$ cells/well) simultaneously using Lipofectamine® 3000 (Thermo Fisher Scientific, Inc.) for 48 h at 37˚C, according to the manufacturer's protocol. Cells were used in subsequent experiments a total of 48 h post-transfection.

Cell Counting Kit-8 (CCK-8) assay. H1975 cells were seeded into 96-well plates at a density of $3x10^3$ cells/well and were incubated at 37˚C for 24 h. The cells were then transfected with siRNA-NC, siRNA-S100A16, Ov-NC or Ov-MOV10. After incubation for 48 h, 10 μl CCK-8 solution (Dojindo Laboratories, Inc.) was added to each well. After a 2-h incubation, the absorbance was measured at 450 nm using a microplate reader (Shanghai Aolu Biological Technology Co., Ltd.).

5-Ethynyl-2'-deoxyuridine (EDU) staining. Cell proliferation was measured using the iClick™ EDU Andy Fluor 555 Imaging Kit (GeneCopoeia, Inc.). H1975 cells ($5x10^4$ cells/well) were seeded into 96-well plates and incubated at 37˚C for 24 h. The cells were then transfected with siRNA-NC, siRNA-S100A16, Ov-NC or Ov-MOV10. A total of 48 h after transfection, the cells in each well were treated with 20 μM EDU for 2 h, according to the manufacturer's instructions. Subsequently, the cells were incubated with 4% paraformaldehyde fixing solution for 30 min followed by 0.5% Triton X-100 permeabilizing solution for 15 min at room temperature. DAPI was used to stain the nuclei at 37˚C for 30 min. The EdU^+ cells were finally observed under a fluorescence microscope (Olympus Corporation).

Wound healing assay. A total of 48 h after transfection, the transfected H1975 cells were seeded into 6-well plates ($5x10^5$ cells/well) and were cultured routinely. After reaching 90% confluence, a wound was made to the cell monolayer using a 200-μl micropipette tip. After washing three times with PBS, the cells were incubated with the serum-free DMEM at 37˚C with 5% CO_2 for 24 h. The cell migration distance was documented under a light microscope (Olympus Corporation). The width of the scratch at 24 h was calculated as a percentage of the width at 0 h using ImageJ software (version 1.4; National Institutes of Health).

Transwell assay. After transfection, H1975 cells ($5x10^4$ cells/well) resuspended in serum-free medium were seeded into the upper chambers of a 24-well Transwell plate (pore size, 8 μm; Corning, Inc.), which had been coated with Matrigel (Becton Dickinson and Company) overnight at 37˚C. The lower chambers were filled with 500 μl medium containing 10% FBS. After 24 h, the remaining cells in the top surface of the insert were removed with a cotton swab, whereas the cells that had invaded to the bottom of the membrane were fixed with 100% methanol for 10 min at 37˚C and stained with crystal violet solution (0.1%) for 15 min at 37˚C, before being subjected to a light microscopic inspection (Olympus Corporation).

Tube formation assay. Matrigel was added to each well of 96-well plates and the entire bottom surface of the well was gently covered. Subsequently, the plates were incubated at 37˚C for 30-60 min to allow the Matrigel to solidify. Finally, eighth passage of HUVECs ($3x10^4$ cells/well) were seeded into the 96-well Matrigel-coated plates and cultured in the presence of DMEM from H1975 cells transfected with different siRNAs/Ov plasmids at 37˚C in a 5% CO_2 incubator for 24 h. Tubules were observed under an inverted light microscope (Olympus Corporation).

Reverse transcription-quantitative PCR (RT-qPCR). After the total RNA was isolated from H1975 cells using TRIzol®

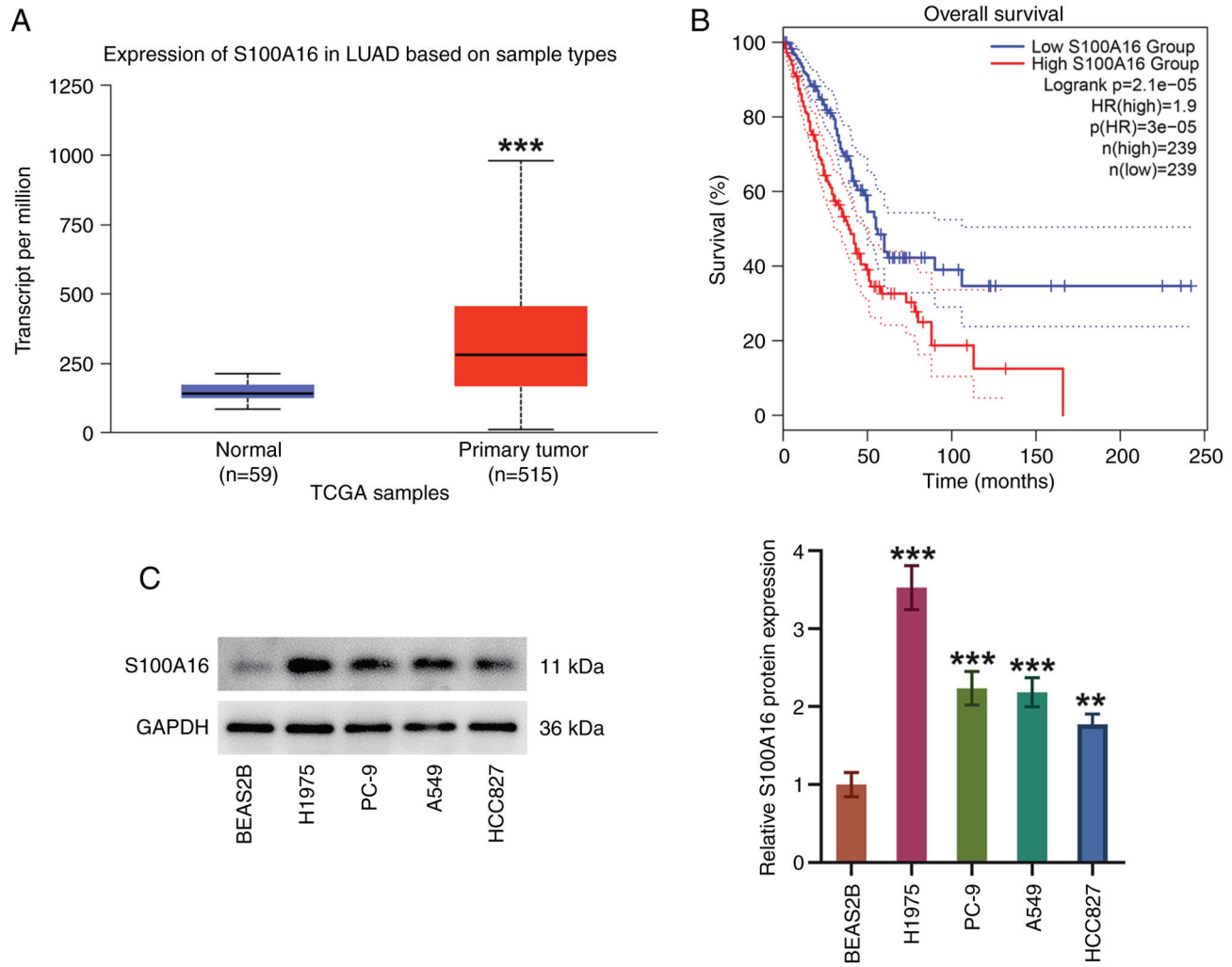

Figure 1. S100A16 is upregulated in LUAD tissues and cells. (A) S100A16 expression in LUAD tissues was analyzed using the UALCAN database. ***P<0.001 vs. Normal. (B) Association of S100A16 expression with the overall survival rate of patients with LUAD. (C) Western blotting was used to examine S100A16 expression in LUAD cells. **P<0.01, ***P<0.001 vs. BEAS2B cells. LUAD, lung adenocarcinoma; S100A16, S100 calcium-binding protein A16; TCGA, The Cancer Genome Atlas.

reagent (Invitrogen; Thermo Fisher Scientific, Inc.), cDNA was generated by RT using a ProSTAR First-Strand RT-PCR kit (Stratagene; Agilent Technologies, Inc.) according to the manufacturer's protocol. qPCR analysis was conducted on the ABI 7500 Real-Time PCR system (Applied Biosystems; Thermo Fisher Scientific, Inc.) using SYBR Green PCR Master Mix Reagents (Takara Bio, Inc.) in accordance with the manufacturer's protocol. The following thermocycling conditions were used: Initial denaturation at 95˚C for 10 min; followed by 35 cycles of denaturation at 95˚C for 15 sec, annealing at 60˚C for 1 min and extension of 10 min at 65˚C. The relative expression levels were calculated based on the $2^{-\Delta\Delta Cq}$ method (18). GAPDH was used as the housekeeping control. The following primers were used for qPCR: ITGA3, forward 5'-CCCAGAGGACCAAGGAAACC-3', reverse 5'-CTCCTGGCTCAGCAAGAACA-3'; GAPDH, forward 5'-AATGGGCAGCCGTTAGGAAA-3', reverse 5'-GCGCCCAATACGACCAAATC-3'.

Western blotting. Following the homogenization of BEAS2B cells, LUAD cells or HUVECs [HUVECs were treated with the conditioned medium (CM) from H1975 cells transfected with different siRNAs/Ov plasmids at 37˚C for 24 h] in RIPA buffer (Epizyme Biomedical Technology Co., Ltd.), protein samples were quantified using the BCA method (Epizyme Biomedical Technology Co., Ltd.) and were separated by SDS-PAGE on 12% gels, before being transferred to PVDF membranes. The membranes were then incubated with 5% BSA (Beyotime Institute of Biotechnology) for 1.5 h at room temperature for non-specific blocking, followed by immunoblotting with primary antibodies specific to S100A16 (cat. no. ab240572; 1:1,000; Abcam), matrix metallopeptidase (MMP)2 (cat. no. ab92536; 1:1,000; Abcam), MMP9 (cat. no. ab76003; 1:1,000; Abcam), vascular endothelial-derived growth factor (VEGF; cat. no. ab46154; 1:1,000; Abcam), VEGF receptor-2 (VEGFR2; cat. no. 26415-1-AP; 1:2,000; Proteintech Group, Inc.), MOV10 (cat. no. ab189919; 1:1,000; Abcam), ITGA3 (cat. no. ab131055; 1:1,000; Abcam), SRC (cat. no. ab133283; 1:1,000; Abcam) and phosphorylated (p)-SRC (cat. no. ab185617; 1:5,000; Abcam) at 4˚C overnight. The membranes were then probed with an HRP-conjugated secondary antibody (cat. no. ab6721; 1:10,000; Abcam) at room temperature for 1.5 h. Anti-GAPDH antibody (cat. no. ab128915; 1:10,000; Abcam)

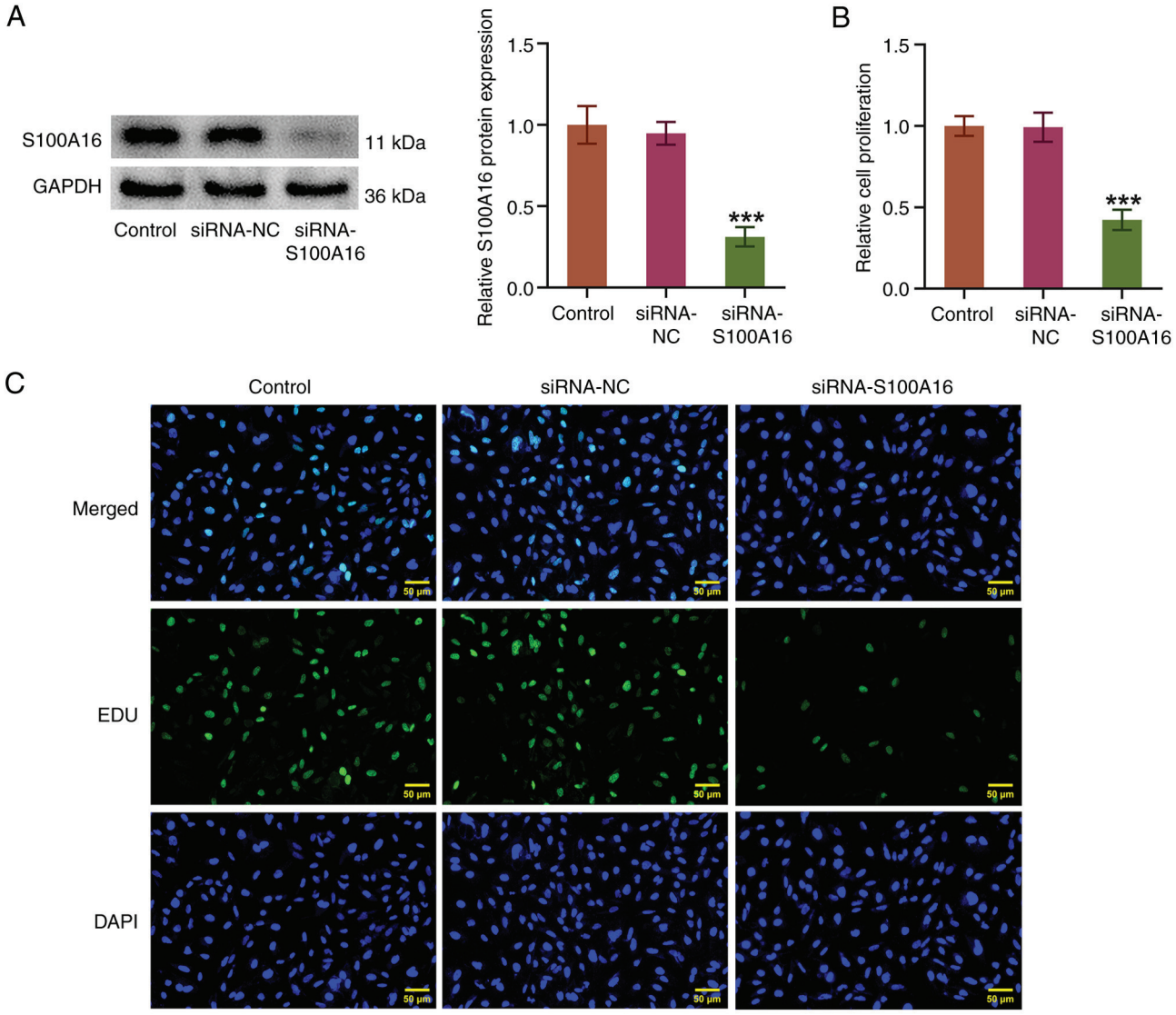

Figure 2. S100A16 knockdown obstructs the proliferation of H1975 cells. (A) Transfection efficacy of siRNA-S100A16 was detected by western blotting. (B) Cell Counting Kit-8 and (C) EDU assays were used to assess cell proliferation. ***P<0.001 vs. siRNA-NC. EDU, 5-ethynyl-2'-deoxyuridine; NC, negative control; S100A16, S100 calcium-binding protein A16; siRNA, small interfering RNA.

was used to confirm equal loading. Blots were at least run in tandem, under the same conditions. Visualization of the blots was conducted using an ECL reagent (Epizyme Biomedical Technology Co., Ltd.) and gray value analysis was performed with ImageJ software (version 1.4).

Co-immunoprecipitation (Co-IP) assay. The Co-IP assay was conducted utilizing a Co-IP kit (cat. no. 26149; Pierce; Thermo Fisher Scientific, Inc.). Following lysis in RIPA lysis buffer (Beyotime Institute of Biotechnology), the H1975 cells were prepared by centrifugation at 14,000 x g and 4˚C for 10 min. The IP was conducted using 2 μg S100A16 (cat. no. ab240572; Abcam), MOV10 (cat. no. ab80613; Abcam) or anti-rabbit IgG (cat. no. ab172730; Abcam) antibodies, after which 20 μl protein A/G agarose beads (Pierce; Thermo Fisher Scientific, Inc.) were added to isolate the protein complexes. The beads were washed with PBS and then boiled to release the bound proteins, which were subjected to SDS-PAGE and western blotting as aforementioned.

RNA immunoprecipitation (RIP) assay. The RIP assay was conducted utilizing the EZ-Magna RIP kit (cat. no. 17-701; MilliporeSigma) according to the manufacturer's protocol. Following lysis in RIPA lysis buffer (Beyotime Institute of Biotechnology), the H1975 cells were treated with RIP buffer containing magnetic beads (MilliporeSigma) conjugated with MOV10 (cat. no. ab80613; Abcam) or IgG (cat. no. ab172730; Abcam) antibodies. Finally, the isolated RNA complexes were subjected to qPCR analysis as aforementioned.

Actinomycin D assay. A total of 48 h after transfection, H1975 cells seeded into 6-well plates ($2x10^5$ cells/well) were treated with 5 μg/ml actinomycin D (GlpBio Technology, Inc.) for 0, 6, 12 and 18 h at 37˚C to examine the stability of ITGA3 mRNA. The remaining ITGA3 mRNA extracted from treated H1975 cells was determined by qPCR analysis as aforementioned.

Statistical analysis. All data are presented as the mean ± standard error of mean and were analyzed with GraphPad Prism

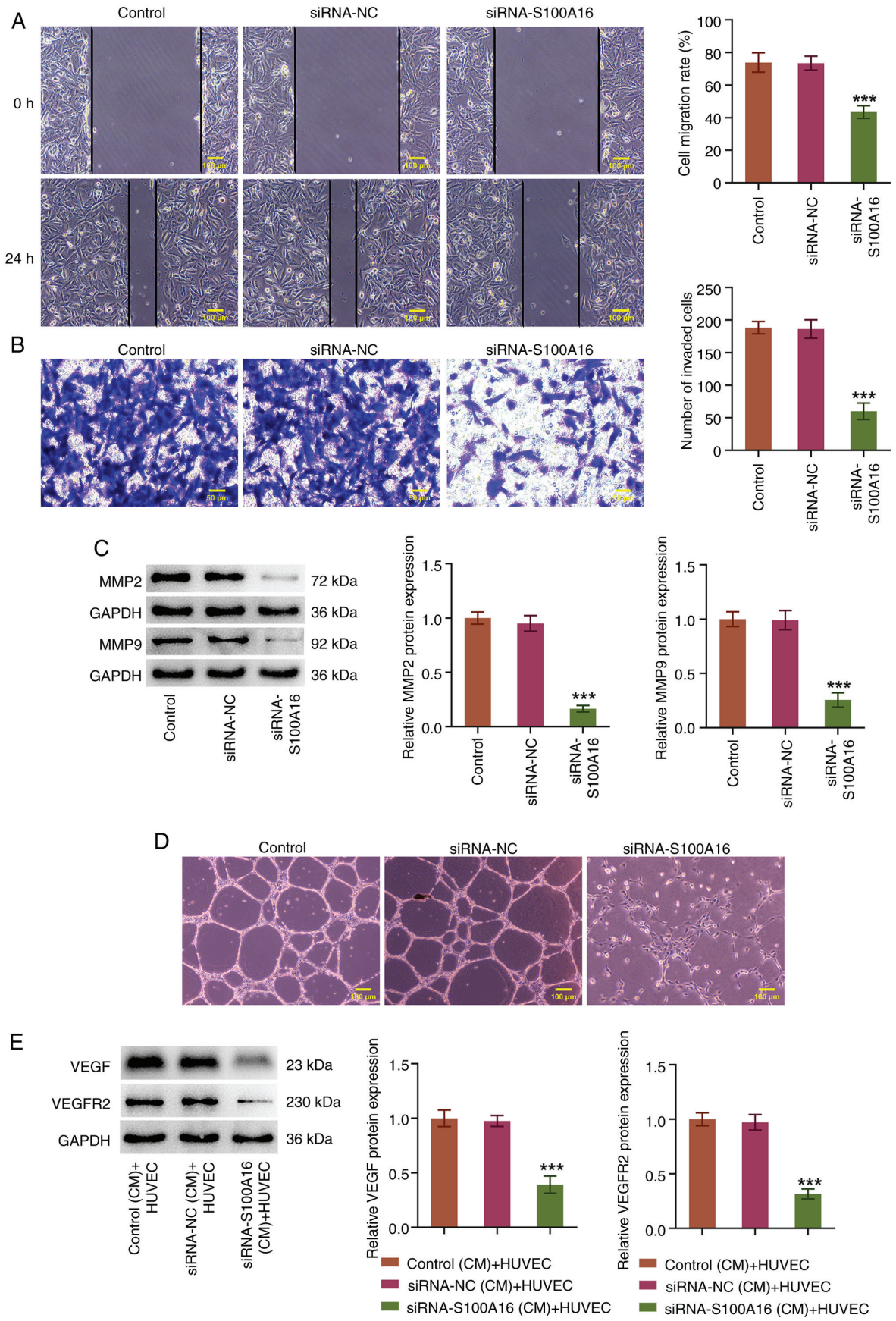

Figure 3. S100A16 knockdown obstructs the migration, invasion and angiogenesis of H1975 cells. (A) Wound healing and (B) Transwell assays were used to evaluate cell migration and invasion, respectively. (C) Western blotting was used to examine MMP2 and MMP9 expression. (D) Tube formation assays were used to estimated cell angiogenesis. ***P<0.001 vs. siRNA-NC. (E) Western blotting was used to examine VEGF and VEGFR2 expression in HUVECs. ***P<0.001 vs. siRNA-NC (CM) + HUVEC. CM, conditioned medium; HUVEC, human umbilical vein endothelial cell; MMP, matrix metallopeptidase; NC, negative control; S100A16, S100 calcium-binding protein A16; siRNA, small interfering RNA; VEGF, vascular endothelial growth factor; VEGFR2, VEGF receptor 2.

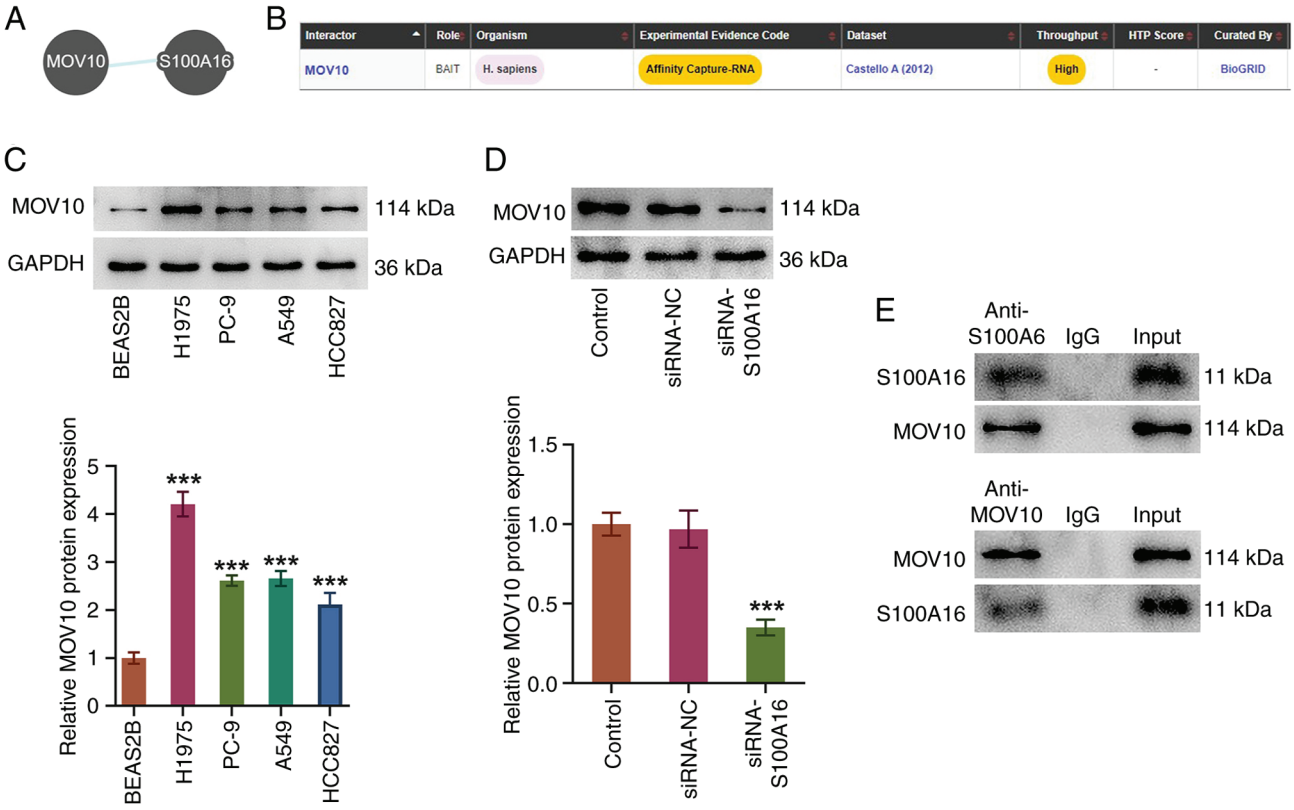

Figure 4. S100A16 interacts with MOV10 in H1975 cells. (A) Pathway Commons and (B) BioGRID databases were used to predict the relationship between S100A16 and MOV10. (C) Western blotting was used to examine MOV10 expression in lung adenocarcinoma cells. ***P<0.001 vs. BEAS2B cells. (D) Western blotting was used to examine MOV10 expression after S100A16 knockdown. ***P<0.001 vs. siRNA-NC. (E) Co-immunoprecipitation assay was used verify the binding between S100A16 and MOV10. MOV10, Mov10 RNA helicase; NC, negative control; S100A16, S100 calcium-binding protein A16; siRNA, small interfering RNA.

8 software (Dotmatics). An unpaired Student's t-test was used to compare two groups, whereas one-way ANOVA followed by Tukey's post hoc test was used to compare three or more groups. P<0.05 was considered to indicate a statistically significant difference.

Results

S100A16 expression is upregulated in LUAD tissues and cell lines. Through UALCAN database analysis, significantly elevated S100A16 expression was observed in LUAD tissues compared with in normal tissues from healthy control individuals (Fig. 1A). Moreover, patients with LUAD were split into high and low expression groups according to median S100A16 expression. High expression of S100A16 predicted a worse overall survival in patients with LUAD (Fig. 1B). S100A16 expression was also examined in cell lines by western blotting, and it was discovered that S100A16 expression levels were higher in LUAD cell lines (H1975, PC-9, A549 and HCC827) compared with those in the BEAS2B cell line (Fig. 1C). H1975 cells exhibited the highest S100A16 expression and were therefore used in subsequent experiments. These findings indicated that S100A16 expression was increased in LUAD and it was associated with an unfavorable outcome in patients with LUAD.

S100A16 knockdown obstructs the proliferation, migration, invasion and angiogenesis of H1975 cells. Post-transfection with siRNA-S100A16, S100A16 expression was markedly depleted (Fig. 2A). The experimental results from the CCK-8 and EDU assays demonstrated that S100A16 knockdown decreased the proliferative ability and the number of EDU^+ H1975 cells compared with that in the siRNA-NC group (Fig. 2B and C). In addition, it was demonstrated that the migratory and invasive capabilities of H1975 cells were reduced when S100A16 was knocked down (Fig. 3A and B). Compared with in the siRNA-NC group, knockdown of S100A16 also resulted in the downregulation of MMP2 and MMP9 expression (Fig. 3C). Furthermore, as shown in Fig. 3D, the CM from H1975 cells with S100A16 knockdown markedly reduced the endothelial capillary-like structures of HUVECs compared with in the siRNA-NC (CM) + HUVEC group (Fig. 3D). Furthermore, the protein expression levels of VEGF and VEGFR2 in HUVECs were downregulated by the CM from H1975 cells with S100A16 knockdown (Fig. 3E). Collectively, these results indicated that knockdown of S100A16 may slow the development of LUAD.

S100A16 interacts with MOV10 in H1975 cells. Through the Pathway Commons and BioGRID databases, it was predicted that MOV10 was a potential target that may bind to S100A16 (Fig. 4A and B). Similarly, MOV10 expression in several LUAD cell lines was assessed, and it was revealed to be elevated in H1975, PC-9, A549 and HCC827 cells compared with that in BEAS2B cells (Fig. 4C). Furthermore, compared with in the siRNA-NC group, MOV10 protein expression

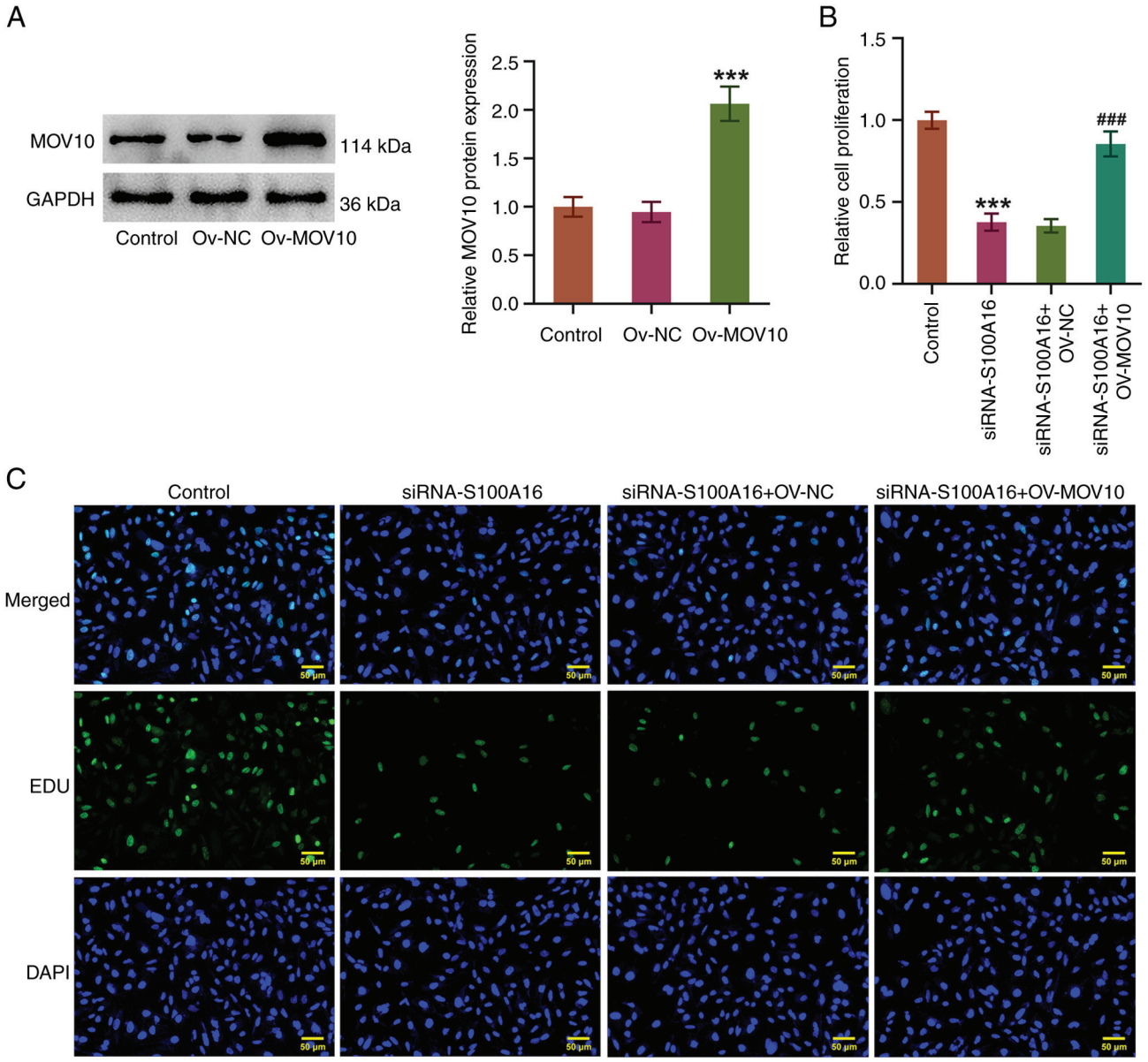

Figure 5. Knockdown of S100A16 suppresses MOV10 expression to hinder the proliferation of lung adenocarcinoma cells. (A) Transfection efficacy of Ov-MOV10 was detected by western blotting. ***P<0.001 vs. Ov-NC. (B) Cell Counting Kit-8 and (C) EDU assays were used to assess cell proliferation. ***P<0.001 vs. Control; ###P<0.001 vs. siRNA-S100A16 + Ov-NC. EDU, 5-ethynyl-2'-deoxyuridine; MOV10, Mov10 RNA helicase; NC, negative control; Ov-MOV10, MOV10 overexpression vector; Ov-NC, empty NC vector; S100A16, S100 calcium-binding protein A16; siRNA, small interfering RNA.

was decreased following knockdown of S100A16 expression (Fig. 4D). Additionally, Co-IP assays demonstrated that S100A16 and MOV10 were both co-immunoprecipitated by MOV10 and S100A16 antibodies, suggesting an interaction between S100A16 and MOV10 (Fig. 4E).

Knockdown of S100A16 suppresses MOV10 expression to hinder the progression of LUAD. To further confirm the relationship between S100A16 and MOV10 in LUAD cells, the Ov-MOV10 plasmid was transfected into H1975 cells. Post-transfection with Ov-MOV10, MOV10 expression was significantly increased compared with that in the Ov-NC group (Fig. 5A). In addition, it was demonstrated that the diminished proliferation of H1975 cells induced by S100A16 knockdown was accelerated again by MOV10 overexpression (Fig. 5B and C). Moreover, S100A16 knockdown markedly reduced the migration and invasion of H1975 cells, accompanied by a decrease in MMP2 and MMP9 expression, whereas these effects were reversed by MOV10 overexpression (Fig. 6A-C). Concurrently, the angiogenic ability of HUVECs was attenuated by knockdown of S100A16; this was also evidenced by the decreased expression levels of VEGF and VEGFR2. By contrast, the angiogenic ability, and the expression levels of VEGF and VEGFR2, were increased in HUVECs in the siRNA-S100A16 + Ov-MOV10 (CM) + HUVEC group compared with those in the siRNA-S100A16 + Ov-NC (CM) + HUVEC group (Fig. 6D and E). In summary, MOV10 overexpression reversed the suppressive effects of S100A16 knockdown on the aggressiveness of LUAD.

S100A16 modulates the ECM-receptor interaction pathway by regulating MOV10-mediated ITGA3 mRNA stability.

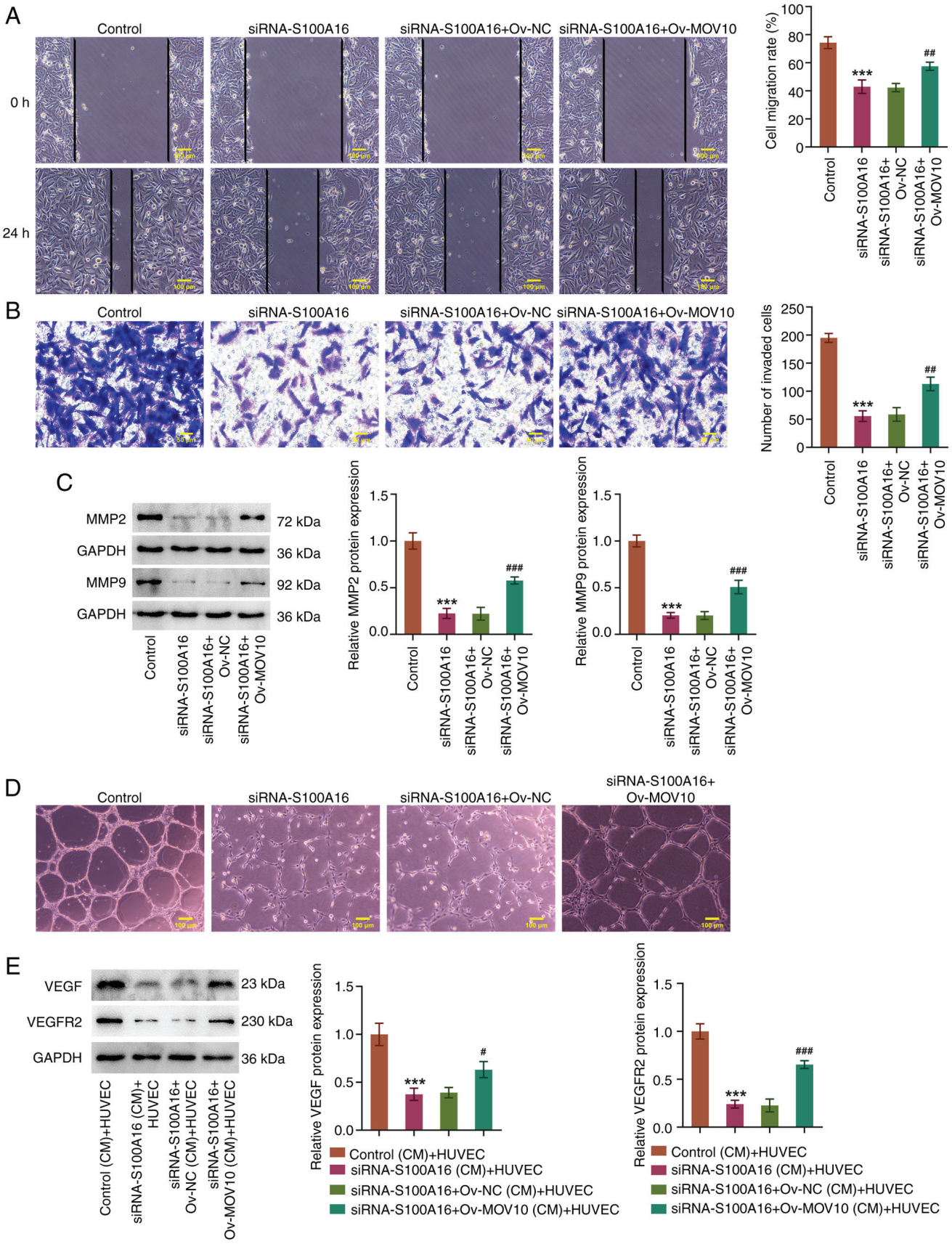

Figure 6. Knockdown of S100A16 suppresses MOV10 expression to hinder the migration, invasion and angiogenesis of lung adenocarcinoma cells. (A) Wound healing and (B) Transwell assays were used to evaluate cell migration and invasion, respectively. (C) Western blotting was used to examine MMP2 and MMP9 expression. (D) Tube formation assays were used to estimate cell angiogenesis. ***P<0.001 vs. Control; $^{\#\#}$P<0.01, $^{\#\#\#}$P<0.001 vs. siRNA-S100A16 + Ov-NC. (E) Western blotting was used to examine VEGF and VEGFR2 expression in HUVECs. ***P<0.001 vs. Control (CM) + HUVEC; $^{\#}$P<0.05, $^{\#\#\#}$P<0.001 vs. siRNA-S100A16 + Ov-NC (CM) + HUVEC. CM, conditioned medium; HUVEC, human umbilical vein endothelial cell; MMP, matrix metallopeptidase; MOV10, Mov10 RNA helicase; NC, negative control; Ov-MOV10, MOV10 overexpression vector; Ov-NC, empty NC vector; S100A16, S100 calcium-binding protein A16; siRNA, small interfering RNA; VEGF, vascular endothelial growth factor; VEGFR2, VEGF receptor 2.

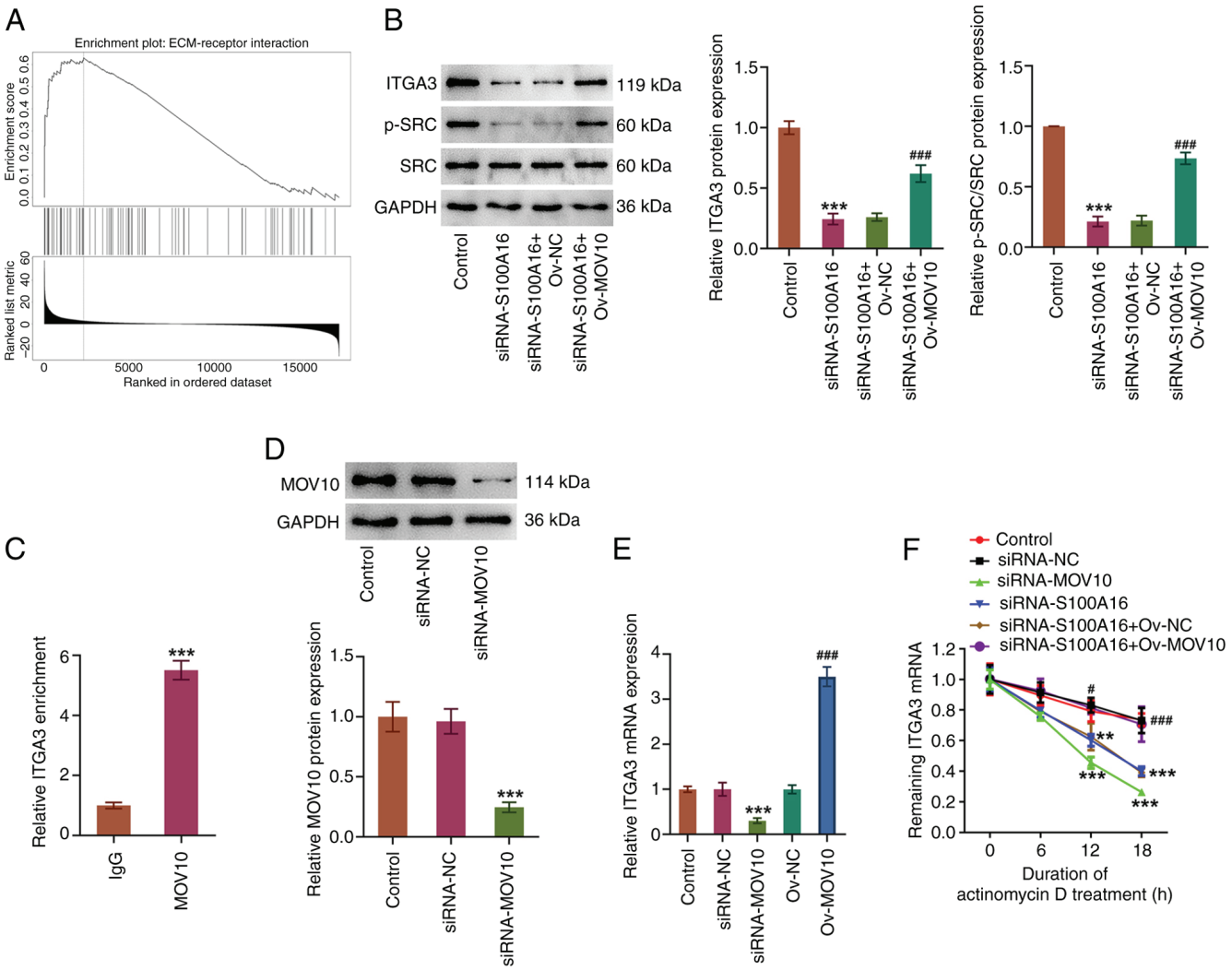

Figure 7. S100A16 modulates the ECM-receptor interaction pathway via regulating the MOV10-mediated ITGA3 mRNA stability. (A) LinkedOmics database was used to predict the enrichment of S100A16 in the ECM-receptor interaction pathway. (B) Western blotting was used to examine ITGA3, p-SRC and SRC expression. ***P<0.001 vs. Control; ###P<0.001 vs. siRNA-S100A16 + Ov-NC. (C) RNA immunoprecipitation assay was used to detect the abundance of ITGA3 mRNA pulled down with the MOV10 antibody. ***P<0.001 vs. IgG. (D) Transfection efficacy of siRNA-MOV10 was detected by western blotting. (E) Reverse transcription-quantitative PCR analysis of ITGA3 mRNA expression after MOV10 was knocked down or overexpressed. ***P<0.001 vs. siRNA-NC; ###P<0.001 vs. Ov-NC. (F) Actinomycin D assay was used to detect ITGA3 mRNA stability. **P<0.01, ***P<0.001 vs. siRNA-NC; #P<0.05, ###P<0.001 vs. siRNA-S100A16 + Ov-NC. ECM, extracellular matrix; ITGA3, integrin α3; MOV10, Mov10 RNA helicase; NC, negative control; Ov-MOV10, MOV10 overexpression vector; Ov-NC, empty NC vector; p-, phosphorylated; S100A16, S100 calcium-binding protein A16; siRNA, small interfering RNA.

Notably, as depicted by the LinkedOmics database, S100A16 was enriched in the 'ECM-receptor interaction' Kyoto Encyclopedia of Genes and Genomes pathway in LUAD cells (Fig. 7A). S100A16 knockdown significantly decreased the expression levels of ITGA3 and p-SRC/SRC, which were both increased by MOV10 overexpression (Fig. 7B). Furthermore, a high abundance of ITGA3 mRNA was pulled down by the MOV10 antibody (Fig. 7C), implying that MOV10 had a high affinity for ITGA3 mRNA. Notably, following MOV10 knockdown in H1975 cells (Fig. 7D), ITGA3 mRNA expression was decreased, whereas it was increased in response to MOV10 overexpression (Fig. 7E). Additionally, the results of the actinomycin D assay demonstrated that MOV10 or S100A16 knockdown decreased the stability of ITGA3 mRNA (Fig. 7F). However, compared with in the siRNA-S100A16 + Ov-NC group, MOV10 overexpression increased the stability of ITGA3 mRNA. Overall, these results indicated that S100A16 interacted with MOV10 to stabilize ITGA3 mRNA and subsequently regulate the ECM-receptor interaction pathway.

Discussion

Previous studies have indicated that intricate biological processes involving genetic and epigenetic alterations have a key role in tumorigenesis (19,20). The S100 protein family has a significant role in the regulation of multiple cancer-related cellular processes, including cell proliferation, differentiation, migration, invasion and epithelial-mesenchymal transition (9). Previous studies have reported that S100A16 may serve as an effective prognostic indicator for various types of cancer, such as bladder (21), pancreatic (22) and colorectal (10) cancer, and LUAD (11,23). In the present study, using bioinformatics analysis, S100A16 expression was predicted to be increased in LUAD tissues, which might

be associated with the low overall survival rate of patients with LUAD. Emerging studies have identified the oncogenic potential of S100A16 in the majority of cancer types, such as by driving cell proliferation, migration and invasion (24-26). In the present study, further investigation showed that S100A16 knockdown hampered the proliferation, migration and invasion of H1975 cells, which was consistent with the study by Wu *et al* (13), in which it was demonstrated that S100A16 accelerated cell proliferation and metastasis in LUAD. MMPs are considered critical regulators in tumor invasion and metastasis, since they are capable of disrupting the ECM and vascular basement membrane of tumor cells, conferring the invasive ability of these cells to the basement membrane, and resulting in tumor cell migration and invasion (27,28). In the present study, it was discovered that, after S100A16 expression was knocked down, the expression levels of MMP2 and MMP9 were also decreased. Accordingly, the anti-proliferative, anti-invasive and anti-migratory roles of S100A16 inhibition in LUAD cells were affirmed.

Angiogenesis is the process by which new blood vessels form from pre-existing blood vessels (29). Moreover, angiogenesis has been well established as a prerequisite for tumor progression and metastasis, through providing oxygen and nutrients to cancer cells and supplying a route for cancer cell metastasis (30,31). Additionally, the association of high angiogenic activity with advanced tumor growth and metastasis in LUAD has been previously demonstrated (32,33). VEGF is a key regulator of angiogenesis that typically exerts its biological effects by binding to its receptors (34). VEGF and VEGFR2 have been shown to be primarily expressed in lung cancer cells, and to be closely linked to the occurrence, development and metastasis of lung cancer (35). Furthermore, previous evidence has demonstrated that S100A16 knockdown can inhibit angiogenesis, and decrease VEGF and VEGFR2 expression in renal cancer cells (25). In the present study, the experimental data highlighted the inhibitory role of S100A16 knockdown in the angiogenesis of HUVECs, as manifested by the decrease in endothelial capillary-like structures, and the downregulation of VEGF and VEGFR2 expression.

Interactions among proteins are central to diversified biological processes, the dysfunction of which is also implicated in the pathogenesis of cancer (36). In the present study, the Pathway Commons and BioGRID databases predicted that MOV10 was a potential protein that may bind to S100A16, which was further verified by Co-IP assay. In addition, it was observed that MOV10 protein expression was decreased after S100A16 expression was knocked down. MOV10 is a novel RBP, the expression of which has been reported to be 2-3 times higher in cancer cells than that in normal cells (14). Additionally, it has been indicated that MOV10 may act as an oncogene in several types of human cancer (37,38). Particularly, high MOV10 expression has been implicated in the poor prognosis of LUAD (15), and has been shown to mediate cell viability, migration and angiogenesis in glioma (39). On this basis, it was further delineated that MOV10 expression was upregulated in LUAD cells, and that overexpression of MOV10 partially reversed the effects of S100A16 knockdown on the proliferation, migration, invasion and angiogenesis of H1975 cells.

RBPs serve an important role in the regulation of mRNA stability and translation at the post-transcriptional level through binding with mRNAs in cancer (40). As predicted by the ENCORI database in the present study, ITGA3 mRNA may be a downstream target of MOV10. The findings of the present study demonstrated that a high abundance of ITGA3 mRNA was pulled down by the MOV10 antibody, and that MOV10 knockdown reduced both the mRNA stability and expression of ITGA3 in LUAD cells, suggesting a notable interaction between MOV10 and ITGA3 mRNA. ITGA3 is a member of the integrin family that can interact with ECM proteins as a cell surface adhesion molecule (41). Focal adhesions are assemblies of cell-ECM linkages mediated by integrin, causing a cascade activation of focal adhesion kinase and SRC (42). Compelling evidence has suggested that inactivation of SRC signaling by ING3 can inhibit the malignant progression of LUAD (43). A recent study has also demonstrated that early-stage lung cancer may be driven by a transitional cell state dependent on a KRAS/ITGA3/SRC axis (44). Accumulating reports have indicated that ITGA3 may be a potential predictor of prognosis in NSCLC (16), and could contribute to invasion and angiogenesis in nasopharyngeal carcinoma (45). In the present study, the LinkedOmics database was used to predict that S100A16 was highly enriched in the ECM-receptor interaction pathway in LUAD cells, and knockdown of S100A16 expression was shown to decrease the expression levels of ITGA3 and p-SRC/SRC, which were increased following MOV10 overexpression.

Notably, there are some limitations in the present study. First, only S100A16 knockdown without S100A16 overexpression was used to detect the effects of S100A16 on MOV10 and the malignant properties of LUAD cells. Second, only one LUAD cell line was used to explore the malignant properties of these cells, and other cell lines should be included in future investigation. Finally, future studies should aim to analyze the effects of ITGA3 on the proliferation and migration of LUAD cells, which were not assessed in the present study.

In conclusion, the present study demonstrated that S100A16 can facilitate cell proliferation, migration, invasion and angiogenesis in LUAD, most likely as a result of increased ITGA3 mRNA stability and regulation of the ECM-receptor interaction pathway via binding to MOV10. The present study supports the significance of S100A16 in LUAD, which may provide value for LUAD therapy.

Acknowledgements

Not applicable.

Funding

No funding was received.

Availability of data and materials

The data generated in the present study may be requested from the corresponding author.

Authors' contributions

LY and ZZ contributed to the conception and design of the present study. LY and AS analyzed the data and drafted the manuscript. AS and RW generated the figures. LY, AS, RW and ZZ conducted the experiments. ZZ reviewed and edited the manuscript. All authors read and approved the final version of

the manuscript. LY and ZZ confirm the authenticity of all the raw data.

Ethics approval and consent to participate

Not applicable.

Patient consent for publication

Not applicable.

Competing interests

The authors declare that they have no competing interests.

References

1. Ferlay J, Colombet M, Soerjomataram I, Parkin DM, Piñeros M, Znaor A and Bray F: Cancer statistics for the year 2020: An overview. Int J Cancer: Apr 5, 2021 (Epub ahead of print).
2. Cao M and Chen W: Epidemiology of lung cancer in China. Thorac Cancer 10: 3-7, 2019.
3. Skřičková J, Kadlec B, Venclíček O and Merta Z: Lung cancer. Cas Lek Cesk 157: 226-236, 2018.
4. Myers DJ and Wallen JM: Lung adenocarcinoma. In: StatPearls. StatPearls Publishing, Treasure Island, FL, 2023.
5. Blandin Knight S, Crosbie PA, Balata H, Chudziak J, Hussell T and Dive C: Progress and prospects of early detection in lung cancer. Open Biol 7: 170070, 2017.
6. Huang P, Zhu S, Liang X, Zhang Q, Liu C and Song L: Revisiting lung cancer metastasis: Insight from the functions of long non-coding RNAs. Technol Cancer Res Treat 20: 15330338211038488, 2021.
7. Slim A, Kamoun H, Hadidene Y, Smadhi H, Meddeb A and Megdiche ML: Postoperative recurrence of primary lung cancer: Anatomo-clinical and therapeutic study. Tunis Med 99: 560-568, 2021.
8. Bresnick AR, Weber DJ and Zimmer DB: S100 proteins in cancer. Nat Rev Cancer 15: 96-109, 2015.
9. Basnet S, Vallenari EM, Maharjan U, Sharma S, Schreurs O and Sapkota D: An update on S100A16 in human cancer. Biomolecules 13: 1070, 2023.
10. Sun X, Wang T, Zhang C, Ning K, Guan ZR, Chen SX, Hong TT and Hua D: S100A16 is a prognostic marker for colorectal cancer. J Surg Oncol 117: 275-283, 2018.
11. Saito K, Kobayashi M, Nagashio R, Ryuge S, Katono K, Nakashima H, Tsuchiya B, Jiang SX, Saegusa M, Satoh Y, *et al*: S100A16 is a prognostic marker for lung adenocarcinomas. Asian Pac J Cancer Prev 16: 7039-7044, 2015.
12. Katono K, Sato Y, Kobayashi M, Nagashio R, Ryuge S, Igawa S, Ichinoe M, Murakumo Y, Saegusa M and Masuda N: S100A16, a promising candidate as a prognostic marker for platinum-based adjuvant chemotherapy in resected lung adenocarcinoma. Onco Targets Ther 10: 5273-5279, 2017.
13. Wu C, Yang J, Lin X, Li R and Wu J: miR-508-5p serves as an anti-oncogene by targeting S100A16 to regulate AKT signaling and epithelial-mesenchymal transition process in lung adenocarcinoma cells. Am J Med Sci 365: 520-531, 2023.
14. Nakano M, Kakiuchi Y, Shimada Y, Ohyama M, Ogiwara Y, Sasaki-Higashiyama N, Yano N, Ikeda F, Yamada E, Iwamatsu A, *et al*: MOV10 as a novel telomerase-associated protein. Biochem Biophys Res Commun 388: 328-332, 2009.
15. Mao CG, Jiang SS, Shen C, Long T, Jin H, Tan QY and Deng B: BCAR1 promotes proliferation and cell growth in lung adenocarcinoma via upregulation of POLR2A. Thorac Cancer 11: 3326-3336, 2020.
16. Li Q, Ma W, Chen S, Tian EC, Wei S, Fan RR, Wang T, Zhou C and Li T: High integrin α3 expression is associated with poor prognosis in patients with non-small cell lung cancer. Transl Lung Cancer Res 9: 1361-1378, 2020.
17. Chandrashekar DS, Bashel B, Balasubramanya SAH, Creighton CJ, Ponce-Rodriguez I, Chakravarthi BVSK and Varambally S: UALCAN: A portal for facilitating tumor subgroup gene expression and survival analyses. Neoplasia 19: 649-658, 2017.
18. Livak KJ and Schmittgen TD: Analysis of relative gene expression data using real-time quantitative PCR and the 2(-Delta Delta C(T)) method. Methods 25: 402-408, 2001.
19. Recillas-Targa F: Cancer epigenetics: An overview. Arch Med Res 53: 732-740, 2022.
20. Kanwal R, Gupta K and Gupta S: Cancer epigenetics: An introduction. Methods Mol Biol 1238: 3-25, 2015.
21. Katsumata H, Matsumoto K, Yanagita K, Shimizu Y, Hirano S, Kitajima K, Koguchi D, Ikeda M, Sato Y and Iwamura M: Expression of S100A16 is associated with biological aggressiveness and poor prognosis in patients with bladder cancer who underwent radical cystectomy. Int J Mol Sci 24: 14536, 2023.
22. Chen T, Xia DM, Qian C and Liu SR: Integrated analysis identifies S100A16 as a potential prognostic marker for pancreatic cancer. Am J Transl Res 13: 5720-5730, 2021.
23. Chen D, Luo L and Liang C: Aberrant S100A16 expression might be an independent prognostic indicator of unfavorable survival in non-small cell lung adenocarcinoma. PLoS One 13: e0197402, 2018.
24. Fang D, Zhang C, Xu P, Liu Y, Mo X, Sun Q, Abdelatty A, Hu C, Xu H, Zhou G, *et al*: S100A16 promotes metastasis and progression of pancreatic cancer through FGF19-mediated AKT and ERK1/2 pathways. Cell Biol Toxicol 37: 555-571, 2021.
25. Wang N, Wang R, Tang J, Gao J, Fang Z, Zhang M, Shen X, Lu L and Chen Y: Calbindin S100A16 promotes renal cell carcinoma progression and angiogenesis via the VEGF/VEGFR2 signaling pathway. Contrast Media Mol Imaging 2022: 5602011, 2022.
26. You X, Li M, Cai H, Zhang W, Hong Y, Gao W, Liu Y, Liang X, Wu T, Chen F and Su D: Calcium binding protein S100A16 expedites proliferation, invasion and epithelial-mesenchymal transition process in gastric cancer. Front Cell Dev Biol 9: 736929, 2021.
27. Jabłońska-Trypuć A, Matejczyk M and Rosochacki S: Matrix metalloproteinases (MMPs), the main extracellular matrix (ECM) enzymes in collagen degradation, as a target for anticancer drugs. J Enzyme Inhib Med Chem 31: 177-183, 2016.
28. Cabral-Pacheco GA, Garza-Veloz I, Castruita-De la Rosa C, Ramirez-Acuña JM, Perez-Romero BA, Guerrero-Rodriguez JF, Martinez-Avila N and Martinez-Fierro ML: The roles of matrix metalloproteinases and their inhibitors in human diseases. Int J Mol Sci 21: 9739, 2020.
29. Dudley AC and Griffioen AW: Pathological angiogenesis: Mechanisms and therapeutic strategies. Angiogenesis 26: 313-347, 2023.
30. Rajabi M and Mousa SA: The role of angiogenesis in cancer treatment. Biomedicines 5: 34, 2017.
31. Majidpoor J and Mortezaee K: Angiogenesis as a hallmark of solid tumors-clinical perspectives. Cell Oncol (Dordr) 44: 715-737, 2021.
32. Zhou Q, Chen X, Chen Q and Hao L: Analysis of angiogenesis-related signatures in the tumor immune microenvironment and identification of clinical prognostic regulators in lung adenocarcinoma. Crit Rev Eukaryot Gene Expr 33: 1-16, 2023.
33. Onn A, Bar J and Herbst RS: Angiogenesis inhibition and lung-cancer therapy. Lancet Oncol 15: 124-125, 2014.
34. Melincovici CS, Boşca AB, Şuşman S, Mărginean M, Mihu C, Istrate M, Moldovan IM, Roman AL and Mihu CM: Vascular endothelial growth factor (VEGF)-key factor in normal and pathological angiogenesis. Rom J Morphol Embryol 59: 455-467, 2018.
35. Chen H, Cong Q, Du Z, Du Z, Liao W, Zhang L, Yao Y and Ding K: Sulfated fucoidan FP08S2 inhibits lung cancer cell growth in vivo by disrupting angiogenesis via targeting VEGFR2/VEGF and blocking VEGFR2/Erk/VEGF signaling. Cancer Lett 382: 44-52, 2016.
36. Cheng SS, Yang GJ, Wang W, Leung CH and Ma DL: The design and development of covalent protein-protein interaction inhibitors for cancer treatment. J Hematol Oncol 13: 26, 2020.
37. Yang D, Hu Z, Xu J, Tang Y, Wang Y, Cai Q and Zhu Z: MiR-760 enhances sensitivity of pancreatic cancer cells to gemcitabine through modulating Integrin β1. Biosci Rep 39: BSR20192358, 2019.
38. El Messaoudi-Aubert S, Nicholls J, Maertens GN, Brookes S, Bernstein E and Peters G: Role for the MOV10 RNA helicase in polycomb-mediated repression of the INK4a tumor suppressor. Nat Struct Mol Biol 17: 862-868, 2010.

39. He Q, Zhao L, Liu X, Zheng J, Liu Y, Liu L, Ma J, Cai H, Li Z and Xue Y: MOV10 binding circ-DICER1 regulates the angiogenesis of glioma via miR-103a-3p/miR-382-5p mediated ZIC4 expression change. J Exp Clin Cancer Res 38: 9, 2019.
40. Li W, Deng X and Chen J: RNA-binding proteins in regulating mRNA stability and translation: roles and mechanisms in cancer. Semin Cancer Biol 86: 664-677, 2022.
41. Shiota T, Li TC, Nishimura Y, Yoshizaki S, Sugiyama R, Shimojima M, Saijo M, Shimizu H, Suzuki R, Wakita T, *et al*: Integrin α3 is involved in non-enveloped hepatitis E virus infection. Virology 536: 119-124, 2019.
42. Hamidi H and Ivaska J: Every step of the way: integrins in cancer progression and metastasis. Nat Rev Cancer 18: 533-548, 2018.
43. Cheng S, Li M, Zheng W, Li C, Hao Z, Dai Y, Wang J, Zhuo J and Zhang L: ING3 inhibits the malignant progression of lung adenocarcinoma by negatively regulating ITGB4 expression to inactivate Src/FAK signaling. Cell Signal 117: 111066, 2024.
44. Moye AL, Dost AF, Ietswaart R, Sengupta S, Ya V, Aluya C, Fahey CG, Louie SM, Paschini M and Kim CF: Early-stage lung cancer is driven by a transitional cell state dependent on a KRAS-ITGA3-SRC axis. EMBO J 43: 2843-2861, 2024.
45. Tang XR, Wen X, He QM, Li YQ, Ren XY, Yang XJ, Zhang J, Wang YQ, Ma J and Liu N: MicroRNA-101 inhibits invasion and angiogenesis through targeting ITGA3 and its systemic delivery inhibits lung metastasis in nasopharyngeal carcinoma. Cell Death Dis 8: e2566, 2017.